Adult neurogenesis through glial transdifferentiation in a CNS injury paradigm

Sergio Casas-Tintó[1, 2], Nuria García-Guillen[1] Maria Losada-Pérez[1, 3]

1- Instituto Cajal (CSIC). Madrid, Spain

2- Instituto de Investigación de Enfermedades Raras (IIER-ISCIII). Majadahonda, Spain

3- Universidad Complutense de Madrid (UCM). Madrid, Spain

Corresponding authors: M L-P marilosa@ucm.es and S C-T sergio.casas@isciii.es

Abstract

As the global population ages, the prevalence of neurodegenerative disorders is fast increasing. This neurodegeneration as well as other CNS injuries cause permanent disabilities. Thus, generation of new neurons is the rosetta stone in contemporary neuroscience.

Glial cells support central nervous system (CNS) homeostasis through evolutionary conserved mechanisms. Upon damage, glial cells activate an immune and inflammatory response to clear the injury site from debris, and proliferate to restore cell number. This glial regenerative response (GRR) is mediated by the neuropil associated glia (NG) in *Drosophila*, equivalent to vertebrate astrocytes, oligodendrocytes (OL) and oligodendrocyte progenitor cells (OPCs). Here, we examine the contribution of NG lineages and the GRR in response to injury. The results indicate that NG exchanges identities between EG and ALG. Additionally, we found that NG cells undergo transdifferentiation to yield neurons. Moreover, this transdifferentiation increases in injury conditions. Thus, these data demonstrate that glial cells are able to generate new neurons through direct transdifferentiation. The present work makes a fundamental contribution to the CNS regeneration field and describes a new physiological mechanism to generate new neurons.

Key words- glia, brain, reprogramming, damage, regeneration, neuron.

Introduction

Neuronal loss caused by injury or neurodegenerative diseases is irreversible in the Central Nervous System (CNS) of vertebrates. Spinal fractures represent 5-6% of all fractures, and spinal cord damage complicates 16-40% of spinal fractures causing significant impairment to patients (Ding et al., 2022). Moreover, according to the United Nations, the prevalence of neurodegenerative diseases will almost double in the next 20 years. Current therapeutic strategies aim to replace damaged or lost cells through dedifferentiation and transplantation or cell reprogramming of glial cells. Thus, understanding glial cell contribution after CNS damage is relevant to attain its functional recovery (Li et al., 2017).

Glial cells activate inflammatory and proliferative responses upon injury in a process known as Glial Regenerative Response (GRR) (Kato et al., 2018; Losada-Perez, 2018). This response is described in multiple species of vertebrates and invertebrates, and the molecular mechanisms underlying this process are conserved from *Drosophila* to mice or humans (Chandra et al., 2023; Kato et al., 2018, 2015, 2011; Li et al., 2020; Losada-Perez, 2018; Losada-Pérez et al., 2021; Purice et al., 2017; Smith et al., 1987). Glial proliferation is a well-known cellular response upon CNS damage (Chandra et al., 2023; Kato et al., 2015, 2011; Li et al., 2020; Li and Hidalgo, 2020; Purice et al., 2017) however it is not clear how this response contributes to CNS regeneration. In mammals, oligodendrocyte progenitor cells (OPCs or NG2-glia) react giving rise to oligodendrocytes while in *Drosophila,* neuropil associated glia play that role (Losada-Pérez et al., 2021). Upon injury, mammalian OPCs can produce astrocytes and oligodendrocytes (OL) contributing to CNS repair (Kato et al., 2018; Niu et al., 2021). GRR of neuropil glia (NPG) in *Drosophila* larva is modulated by a genetic network that controls the switch between quiescence, proliferation and differentiation. Although, whether these mechanisms operate in the mature differentiated adult brain is still unknown. In *Drosophila*, NPG somata reside in the cortex/neuropil interface (Figure 1A). NPG includes two groups: Astrocyte-Like Glia (ALG), and Ensheathing Glia (EG). EG enwraps the neuropil, and bundles of axons within the neuropil that define different functional regions (Losada-Perez, 2018). By contrast, ALG cells project to the neuropil forming a dense meshwork with the synapses (Losada-Perez, 2018), which suggests that ALG cells may play a significant role in maintaining the architecture and function of the neuropil. Larval ALG upregulates *kon-tiki* expression upon injury, a gene which is required for glial division (Losada-Perez et al., 2016). Besides, larval EG during metamorphosis can de-differentiate, proliferate and re-differentiate into adult ALG and EG (Kato et al., 2020). Thus, NPG appear as good candidates to replace lost cells with functional ones.

We have studied the physiological mechanisms that occur after CNS injury, focusing on the fate of glial cells upon damage. We provide the first evidence of *in vivo* physiological reprogramming of glial cells into other glial identities and into new neurons in the adult brain.

RESULTS

1. Astrocyte-like glia proliferation in adult is increased upon crush injury

Previously we described that glial cells proliferate in basal conditions and in response to crush injury in the adult fly (Losada-Pérez et al., 2021) although we did not identify the glial subtype responsible for this response. Thus, we questioned if those dividing cells were of the NPG type, that is, Astrocyte-Like Glia (ALG), as previous works suggest in larvae (Kato et al., 2020; Losada-Perez et al., 2016), or Ensheathing Glia (EG).

ALG identity is defined by the co-expression of *repo* and *prospero* transcription factors (Omoto et al., 2015). To determine if ALG cells divide upon injury, we caused a crush in the metathoracic neuromere of the adult ventral nerve cord (VNC, Figure 1A) (Losada-Pérez et al., 2021) and performed EdU experiments combined with staining with anti-Repo (pan-glia marker) and anti-Prospero antibodies. The results show that ALG cells (Repo positive, Prospero positive) divide (EdU positive) after injury (Figure 1B). Besides, we also observed EdU+ Repo+ cells that were Pros negative. Therefore, this result indicates that glial cells, different from ALG, also undergo division.

There is no specific nuclear marker for EG cells, consequently, to determine if the other dividing cells were EG, we expressed FLY-FUCCI (Zielke et al., 2014) under control of a specific driver for EG (R56F03-Gal4). This genetic tool allows the visualisation of cell-cycle stages by combinations of fluorescent protein reporters (see Materials and Methods). In parallel, we also expressed FLY-FUCCI under control of the ALG specific driver alrm-Gal4 (Altenhein et al., 2006; Beckervordersandforth et al., 2008).

We quantified the number of ALG or EG cells in G2-M (i.e., GFP and RFP positive) in control and injured animals at 24h after injury. The data show that EG cells have a basal division rate which does not change in response to injury. In contrast, ALG cells have a higher division rate in basal conditions compared to EG, and this rate increases in response to injury (Figure 1C-C'). This result indicates that adult ALG cells activate a proliferative response after injury, akin to the proliferative response in larvae (Losada-Perez et al., 2016). On the other hand, the basal proliferation of EG explains the presence of Repo+EdU+Pros- cells.

To further confirm these results, we generated Twin-MARCM clones (Yu et al., 2009) using specific drivers for EG (R65F03-Gal4) or ALG (alrm-Gal4). We combined the Twin-

MARCM technique with tubGal80^{TS} under temperature control (see Materials and Methods). This technique allowed the study of ALG or EG division selectively in adulthood (Figure 1D).

The results of ALG MARCM clones indicate that ALG divides in normal conditions in the adult CNS. Since ALG cells are very heterogeneous in size and shape we were not able to determine the number of cells that composed each clone (Figure 1D'). However, we quantified the number of individuals with clones. The results indicate that the percentage of samples with clones is significantly higher in injured animals compared to controls (Figure 1E). To confirm that this division is not the result of residual development, we repeated the experiment with *mature* (seven-days-old) flies. In this case, the percentage of not-injured CNS with clones is lower compared with young flies (Figure 1E) indicating we were observing a developmental effect. However, in *mature* flies, the percentage of samples with clones is significantly higher in injured animals compared to not-injured controls (Figure 1E) indicating that ALG divide upon damage after the developmental program is finished.

MARCM clones induction with the specific driver for EG did not generate any clone, neither in normal conditions nor after crush injury. MARCM technique generates clones in a stochastic manner, therefore the lack of MARCM clones does not indicate that EG never divides, instead, it indicates that this event is less frequent than ALG division. These results are consistent with the FLY-FUCCI results.

Altogether, the results indicate that there is a basal division rate of neuropil glia where EG divides less often than ALG. Also, ALG shows a proliferative response to crush injury. These findings go in line with previous reports indicating the proliferative response of glial cells (Kato et al., 2018; Losada-Perez, 2018). Moreover, the results now describe proliferation of adult fully-differentiated glial cells and define a differential response of EG and ALG in basal conditions, and upon injury. OPCs carry the proliferative response upon injury in mammals (Kato et al., 2018; Losada-Perez, 2018). Therefore, these results further support the homology between ALG and vertebrate OPC.

2. Programmed cell dead regulates ALG number after injury

The Twin-MARCM technique implies that the cell division includes homologous recombination. The first division would give rise to two daughter cells, one GFP positive and other RFP positive (Figure 1D). These differentially marked daughter cells could further divide or not, yielding clones of different sizes (Figure 1D' and F). However, during ALG MARCM clone quantification we noticed that >50% of clones were single-colour clones (Figure 1 G-H). This means that after the first division, one of the daughter cells

either dies or changes its identity (as we use the alrm-Gal4 ALG specific driver to express GFP or RFP). To determine if single colour clones could be explained by Programmed Cell Dead (PCD) we inhibited it by co-expressing UAS-p35 (Hay et al., 1994), while inducing Twin-MARCM clones in injured animals. The results showed that p35 significantly reduced the number of single colour clones (Figure 1H). These results indicate that a portion of dividing ALG cells undergo PCD, reducing the final number of newly generated ALG after injury. This cellular behaviour is commonly observed during development, where cells are produced in excess and are eliminated by PCD later (Fuchs and Steller, 2011; Gabilondo et al., 2018; Miguel-Aliaga and Thor, 2009). Now we describe how differentiated glial cells reproduce this proliferative response, and the elimination of cells by PCD.

3. NP glia exchange identities between EG and ALG

Apoptosis inhibition significantly reduces ALG single-colour clones, but we could still observe them. This could be explained by the different effectiveness of the UAS- p35 to suppress apoptosis, but also by the existence of dedifferentiation or transdifferentiation processes. To test this hypothesis, we combined the G-TRACE tool, which allows the visualisation of historical and current Gal4 activation, with TubGal80ts to restrict the G-trace historical visualisation to adulthood.

We drove the expression of G-TRACE reporter with the specific drivers for ALG or EG and analysed the historical and current activation of ALG or EG drivers. The results show that in both ALG and EG experiments there were cells with historical driver activation but not current activation (GFP+RFP-) (Figure 2A-A'). Also, those cells have distinctive nuclear sizes and positions. We named the first type neuropil-like cells (NP-like, arrowheads Figure 2A), as they have similar nuclear shape and size to ALG and EG and they were found in the cortex-neuropil interface, where neuropil glia nuclei are usually positioned. The second type of cells were found in the ventral cortex and presented larger nuclei compared to NP-like cells, thus, given their position we named those cells as Ventral Cortex cells or VC cells (arrowheads Figure 2A').

Next, we asked if those cells that changed their fate still had a glial identity. To answer this question, we stained NP-like cells with the pan-glial marker Repo. The results indicate that NP-like cells are glia as they were Repo+ (Figure 2 B-B'). To confirm this, we expressed G-TRACE under the control of *Repo Gal4* pan-glial driver and analysed the presence or absence of transformed cells. We identified GFP+RFP- cells localised in the ventral cortex with identical nuclear shape as the VC cells identified in previous

experiments (Figure 2C), however, we could not find any NP-like cells. Thus, it seems that NP-like cells have glial identity while VC cells have not.

Next, we addressed if the NP-like glia fate change was triggered by injury. To that end we quantified the number of NP-like cells transformed from ALG or from EG, in not-injured and injured animals 6h and 24h after crush injury. The results show that the number of NP-like cells does not increase in response to injury no matter their initial identity, ALG or EG (Figure 2 D). However, we found significant differences in the number of transformed cells that originated from ALG or EG. We observed that ALG to NP-like transformation is less frequent than EG to NP-like transformation (<0.5% in ALG compared with >10% in EG) (Figure 2E).

The transformation of EG into ALG has been shown during metamorphosis (Kato et al., 2020), indicating the versatility of those cells. Thus, we use anti-prospero to determine if the NP-like cells originated from EG have ALG identity in this context. The images show that the NP-like cells originated from EG where pros+ (Figure 3A), suggesting that EG transdifferentiate into ALG. Next, to determine if Prospero is required for EG to ALG transformation we quantified and compared the number of NP-like cells that arose from EG origin in controls and in individuals where *pros* was downregulated specifically in EG cells. The results showed a significant decrease in the number of NP-like cells upon pros knockdown in EG cells (Figure 3B). These results indicate that *pros* downregulation in EG reduces inter-glia conversion. Thus, we can conclude that Prospero is required for the EG to ALG transformation in adult CNS.

This is the first report of EG to ALG transformation *in vivo* in adult flies. The functional implications of this process include CNS regeneration, cellular homeostasis and behavioural consequences including locomotion recovery, but probably also learning and memory.

4. NP-Glia transdifferentiate to neurons upon injury

Repo-GTRACE experiments demonstrated that VC cells are not glia (Figure 2B-C). To test if these new cells have a neuronal identity, we stained the VNCs with the pan-neuronal marker Elav. The analysis showed that these cells were Elav positive (Figure 4A-A). This result indicates that glial cells can transdifferentiate into neurons under normal conditions. Next, we quantified the number of VC cells following injury. The results show that the number of VC cells is significantly higher in injured animals compared to non-injured controls (Figure 4B). Next, we analysed which NPG

subpopulation (i.e., ALG or EG) were responsible for this increase of VC neurons. To eliminate any developmental effect, we analysed in mature flies (see M&M) the possible trans differentiation from ALG or EG into VC in control and injured animals. The result showed that the new neurons originate from both transdifferentiated ALG and EG (Figure 4C).

So far, we have seen that ALG cells divide upon injury while EG do not. On the other hand, VC neurons increase out from ALG and EG types in response to injury. This could indicate that ALG divides prior to trans differentiation while EG transdifferentiate directly. To test this hypothesis, we quantified the number of ALG and EG cells in both injured animals and not-injured controls. We found a significant increase of ALG number in injured animals compared to controls in line with our previous results. Moreover, we found a significant decrease of EG in injured animals compared to not-injured controls supporting the direct transformation in response to injury (Figure 4D).

Finally, to determine the identity of trans differentiated neurons, we stained VC cells with different neuronal markers such GABA, ChaT or GluRIIA (Boppana et al., 2017; Chen et al., 2016; Katheder et al., 2023; Kolodziejczyk et al., 2008). The images showed that VC cells are negative for all (Figure S1), therefore we weren't able to determine their identity. This result could suggest that these cells are immature.

Taken together, our results indicate that ALG and EG generate new neurons in response to injury through two different mechanisms. ALG divide and transdifferentiate while EG transdifferentiate directly. Thus, glial cells reveal as key contributors to newly generated glia and neurons during regeneration.

Many authors are exploring the potential of astrocytes to generate new neurons, however they are focused on artificial reprogramming or trans differentiation (Talifu et al., 2022). This is the first description of this phenomenon observed *in vivo in wild type animals*. Therefore, these findings open a new approach to generate new neurons in a damaged CNS. Understanding the molecular mechanisms that govern this physiological glial behaviour would have an immeasurable value.

MATERIALS AND METHODS

Fly stocks and genetics

Experiments were performed in adult *Drosophila melanogaster* flies raised at 25°C or combining 17°C with 29°C for temporal control of UAS/Gal-4 using the thermo-sensitive repression system Gal80 TS. Fly stocks used were: *Alrm-Gal4* (BL 67032), *R56F03-Gal4* (BL 39157), *UAS-GFP.E2f*; *UAS-mRFP.CycB* (Fly- FUCCI, BL 55100), *repo-Gal4* (BL-7415), *tub Gal80 ts* (BL-7019), *UAS-p35* (BL5073), UAS-GTRACE (BL 28281), Twin-*MARCM stocks* (BL56184 and BL56185), *UAS-prosRNAi* (BL-26745) form Bloomington

Drosophila Stock Center and *yw hs-FLP* from A. Ferrús. To control the activation of different tools we combined the UAS/Gal4 system with the *Tubulin-Gal80^{TS}* (temperature sensitive) tool. We maintained the desired genotypes at non-permissive temperature (i.e., 17°C, where the Gal80^{TS} repressor protein is active), to block UAS constructs expression.

Crush injury

Crush Injury was performed following the protocol described in Losada-Perez et al. 2021 (Losada-Pérez et al., 2021). When the experiment did not require Gal4/UAS activation exclusively in adult (i.e., UAS Fly-Fucci and Twin-spot MARCM), we breed flies at 25°C; we selected one day old adult flies emerging between 12 to 24h hours before injury; we selected mature flies that emerged 5 to 7 days before injury. In the experiments where we needed to temperature control Gal4 activation (i.e., UAS-GTRACE) we breed flies at 17°C, then we selected that emerged 24 to 48h before injury (for 1-day old flies) or that emerged 10 to 12 days (for mature flies) and then collocated at permissive temperature (i.e., 29° C, where Gal80 TS is inactive and the Gal4/UAS system is active).

Injured flies dragging the third pair of legs that did not show external signs of cuticle damage were selected 24 h later (24 h after crush injury (ACI)).

FLY-FUCCI system

FLY-FUCCI (Zielke et al., 2014) allows the visualization of Cell-cycle activity, GFP or RFP-tagged forms of E2F1 and Cyclin B proteins respectively are expressed using the UAS/Gal4 system. Thus, by the presence/absence of GFP and/RFP it is possible to determine the cell cycle stage. We identify GFP positive, RFP positive cells as cells in the G2-M cell cycle phase.

Twin-spot MARCM *(Mosaic Analysis with a Repressible Cell Marker)*

Using Twin-spot MARCM technique (Yu et al., 2009) it is possible to detect cells dividing in a specific moment. When a cell divides, each of the two resulting cells is marked with GFP or RFP, always considering that the promoter directing this tool gets activated. This is possible because the genetic constructs used within this tool includes a flipase under the control of a heat shock promoter (HsFlp). This enzyme induces mitotic recombination of sequences situated between FRT (Flipase recognition target) sites. To induce flipase activation, flies were exposed to heat-shocks by introducing the vials in 37ºC water baths for 60 minutes.

<u>Twin-MARCM clone induction</u>

We performed two 60-minute-heat shocks in a water bath at 37 ºC to induce Twin-MARCM clones. Vials with one day old flies received the first heat shock right before crush injury. Then, flies were placed at 25 ºC s for 6 hours. After that, flies received the

second heat shock and placed again at 25 ºC. Afterwards, flies were dissected 24h after injury.

G-TRACE tool (*Gal4-Technique for Real-time and Clonal Expression)*

GTRACE tool (Evans et al., 2009) allows the visualization of historical and current expression of *Gal4* gene. It is based on the combination of 3 genetic constructs: *UAS-RFP*, *UAS-FLP* and *Ubi*^{63}*- FRT-Stop-FRT-GFP*.

Whenever *Gal4* expression is activated, it induces the expression of *UAS-RFP* and *UAS-FLP*. Flippase enzyme recognizes *FRT* sites and removes stop sequences, allowing *GFP* constitutive expression (GFP gene is under the control of a constitutive promoter *Ubiquitine-p63E*). Cells expressing *Gal4*, and the posterior lineage, will be marked with GFP. This tool allows tracking the current expression of a *Gal4* enhancer sequence (*UAS-RFP* in red) and its historical expression (*Ubi-GFP* in green).

G-TRACE activation

Animals that develop at 17°C were selected 24 to 48h after emerging and were collocated at permissive temperature (29° C) for 6 hours. Then, the crush injury was performed. Flies were selected and dissected 24h ACI.

EdU incorporation

We used EdU staining to detect cell proliferation. Flies were injured and left overnight in Eppendorf tubes containing EdU solution (100µM EdU in 5% sugar, 1% dye). 24h after injury flies were dissected in cold 4%FA and fixed 15 minutes in 4%FA while rocking and washed twice with 3%BSA in PBS. Fixed VNCs were permeabilized with PBSTx0,5 (1xPBS, 0,5% Triton X-100) for 20 minutes and washed twice again with 3% Bovine serum albumin in PBS. EdU detection was performed by using the Click-iT® reaction cocktail (Click-iT® EdU, Invitrogen). Afterwards, the CNS were immunostained following the protocol described below.

Immunohistochemistry and EdU detection

We performed the immunohistochemistry following the protocol for adult *Drosophila* immunolabeling according to Purice et al. (2017).

We used the following antibodies: mouse anti-Repo (DSHB, 8D12 ID: AB_528448, 1:200), mouse anti-Elav (DSHB, 9F8A9 ID: AB_528217), mouse anti-prospero (DSHB, MR1A, ID: AB_528440), mouse anti-ChAT (DSHB, ID:AB_528122), mouse anti-GluRIIA (DSHB, ID: 528269), guinea pig anti-Repo (gift from B. Altenhein (von Hilchen et al., 2013)), anti-Ph3 (Millipore, 3H10), anti-GABA (Sigma-Aldrich, A2052 (Jackson et al., 1990)).

Quantification, statistical analysis and imaging

Images were acquired by confocal microscopy (LEICA TCS SP5) and processed using Fiji (ImageJ 1.50e) software. Images were assembled using Adobe Photoshop CS4 and Adobe Illustrator CS4. Cells were counted using the cell counter plugin from Fiji or Imaris (Imaris 6.3.1 software- Bitplane). Data were analysed and plotted using GraphPad Prism v7.0.0 or v9.0.0. For qualitative data, analysed in Fig. 1D-D', we performed a binomial test (**P<0.01). For quantitative data, we used a D'Agostino – Pearson normality test and analysed data with normal distributions by using two-tailed t-test with Welch's unequal variances t-test. Error bars represent standard deviation (±s.d.).

Acknowledgements

We thank Professor Alberto Ferrús, Dr Francisco Martín, Professor Agustín Zapata and the anonymous reviewers for critiques of the manuscript and helpful discussions and Carlos Rodriguez and Esther Seco for flystocks maintenance. We are grateful to the Bloomington Drosophila stock Centre and the Developmental Studies HydridomaBank and Benjamin Altenhein for supplying fly stocks and/or antibodies, and FlyBase for its wealth of information. We acknowledge the support of the Confocal Microscopy unit at the Cajal Institute and at ISCIII. Finally, we thank Fundación Jose Maria Lopez Feliú and MICINN (Grants PI22CIII/00062 and PID2022-137751OA-I00) for funding.

Figure legends

FIGURE 1. Neuropil glia proliferation in normal conditions and upon crush injury in adults

A, Schematic representation of Drosophila adult Central Nervous System (CNS) and Ventral Nerve Cord (VNC), indicating the MtN, where the injury is performed. **B,** Representative confocal image showing dividing cells (EdU+) with ALG identity (Repo+ and Pros+) and glial identity different from ALG (Repo+, Pros-). **C**, Number of ALG or EG cells in G2-M per MtN, in normal conditions and 24 h after injury. Paired *t*-test, **P*<0.05, ***P*<0.01. **C'-C''**, Representative images of ALG in G2-M showing their position within the injured area (**C'**) and a magnification showing the detail of GFP+RFP+ cells (**C''**). **D**, Diagram of how the Twin-Spot MARCM tool works. **D'**, Representative confocal image of ALG clones generated with Twin-Spot MARCM. **E**, Number of VNCs with/without clones in controls and Injured VNCs in young (1 day old) and mature (7 day old) animals. Chi-square binomial test, ***P*<0.01, *****P*<0.0001. **F-G**, Representative confocal images of a two-color ALG clone (**F**) and a single-color ALG clone (**G**). **H**,

Percentage of ALG single-color clones in injured controls and Injured VNCs where apoptosis was inhibited in ALG. Unpaired t-test $^{**}P<0.01$. Genotypes: wild type (B); *AlrmGal4>UAS-Fly-FUCCI* (C-C'); *R56F03Gal4>UAS-Fly-FUCCI* (C); *HsFLP; UAS-GFP, UAS-RFP$_{RNAi}$ /UAS-RFP, UAS-GFP$_{RNAi}$; tubGal80ts:alrmGal4;* (D'-H): *HsFLP; UAS-GFP, UAS-RFP$_{RNAi}$ /UAS-RFP, UAS-GFP$_{RNAi}$; tubGal80ts:alrmGal4/UAS-p35* (H). Scale bars: 50 µm (B, C, E); 15 µm (C'', F,G)

FIGURE 2. Neuropil glia transdifferentiate to two different cell types

A-B. Representative confocal slices showing transdifferentiated EG cells with the G-TRACE tool. **A**, Medial slice showing NP-like cells position within the MtN. **B**, Zoom slice (merge and separated channels) showing NP-like cells (GPF+, RFP-) have glial identity (repo+). **A'**, Ventral slice showing VC cells position within the MtN. **B'**, Zoom slice (merge and separated channels) showing VC cells (GPF+, RFP-) are not glia (repo-). **C**, Representative ventral slice showing transdifferentiated CV cells visualised with G-TRACE toll driven by the pan-glial factor Repo-Gal4. **D**, Number of NP-like cells originated from ALG or EG in not injured and injured MtM. Mann Whitney test *ns* $p>0.05$, $^{**}P<0.01$. **E**, Percentage of NP-like cells compared with the total number of NP glia that originate them. Scale bars: 50 µm (A, A', C); 15 µm (B,B'). Genotypes: *tubGal80ts, R56F03Gal4>UAS G-TRACE* (A, B, D, E); *tubGal80ts, repoGal4>UAS G-TRACE* (C); *tubGal80ts, AlrmGal4>UAS G-TRACE* (D, E).

FIGURE 3. EG transdifferentiation into ALG requires prospero

A. Representative image of NP-like cells originated from EG stained with ALG marker Prospero. Top left: Merge image with DAPI. Top right: Merge image without DAPI. Bottom left: GFP signal. Bottom right: RFP signal and pros staining. **B**, Number of NP-like cells originated from EG in controls animals where pros was inhibited in EG. Unpaired t-test $^{*}P<0.05$. Scale bar: 15 µm (A). Genotypes: *tubGal80ts, R56F03Gal4>UAS G-TRACE* (A, B)

FIGURE 4. EG and ALG transdifferentiate into neurons upon injury through two different mechanisms

A-A'.Transdifferentiated VC cells (GFP+,RFP-) raised from ALG (**A**) and EG (**A'**) are elav+. From left to right: Merge with DAPI, merge without DAPI and green and red channels merged. **B**, Number of transdifferentiated glia (VC cells, GFP+, RFP-) in controls and injured VNCs. STATS. **C**, Number of transdifferentiated VC cells (GFP+, RFP-) originates from ALG or EG in controls and injured mature animals. **D**, Number of ALG or EG that remain ALG or EG in controls and injured VNCs. Statistics (B, C, D):

Paired t-test ***p<0.001, **p<0.01, *ns* p>0.05. Scale bar: 15 µm (A). Genotypes: *tubGal80ts, R56F03Gal4>UAS G-TRACE* and *tubGal80ts, AlrmGal4>UAS G-TRACE*

FIGURE S1. New neurons do not co-localize with markers for mature neurons

Representative confocal images of VC cells (GFP+, RFP+) stained with DAPI (grey) and different antibodies in magenta, anti-ChAT (**A**), GluRIIA (**B**) and GABA (**C**). Dotted white circles indicate the VC cells. Scale bar: 15 µm (A). Genotypes: *tubGal80ts, repoGal4>UAS G-TRACE.*

References

Altenhein B, Becker A, Busold C, Beckmann B, Hoheisel JD, Technau GM. 2006. Expression profiling of glial genes during Drosophila embryogenesis. *Dev Biol* **296**:545–560. doi:10.1016/j.ydbio.2006.04.460

Beckervordersandforth RM, Rickert C, Altenhein B, Technau GM. 2008. Subtypes of glial cells in the Drosophila embryonic ventral nerve cord as related to lineage and gene expression. *Mech Dev* **125**:542–557. doi:10.1016/j.mod.2007.12.004

Boppana S, Kendall N, Akinrinsola O, White D, Patel K, Lawal H. 2017. Immunolocalization of the vesicular acetylcholine transporter in larval and adult Drosophila neurons. *Neurosci Lett* **643**:76–83. doi:10.1016/j.neulet.2017.02.012

Chandra B, Voas MG, Davies EL, Roberts-Galbraith RH. 2023. Ets-1 transcription factor regulates glial cell regeneration and function in planarians. *Development* **150**:dev201666. doi:10.1242/dev.201666

Chen Z, Del Valle Rodriguez A, Li X, Erclik T, Fernandes VM, Desplan C. 2016. A Unique Class of Neural Progenitors in the Drosophila Optic Lobe Generates Both Migrating Neurons and Glia. *Cell Rep* **15**:774–786. doi:10.1016/j.celrep.2016.03.061

Ding W, Hu S, Wang P, Kang H, Peng R, Dong Y, Li F. 2022. Spinal Cord Injury: The Global Incidence, Prevalence, and Disability From the Global Burden of Disease Study 2019. *Spine* **47**:1532–1540. doi:10.1097/BRS.0000000000004417

Evans CJ, Olson JM, Ngo KT, Kim E, Lee NE, Kuoy E, Patananan AN, Sitz D, Tran P, Do M-T, Yackle K, Cespedes A, Hartenstein V, Call GB, Banerjee U. 2009. G-TRACE: rapid Gal4-based cell lineage analysis in Drosophila. *Nat Methods* **6**:603–605. doi:10.1038/nmeth.1356

Fuchs Y, Steller H. 2011. Programmed Cell Death in Animal Development and Disease. *Cell* **147**:742–758. doi:10.1016/j.cell.2011.10.033

Gabilondo H, Rubio-Ferrera I, Losada-Pérez M, Del Saz D, León Y, Molina I, Torroja L, W Allan D, Benito-Sipos J. 2018. Segmentally homologous neurons acquire two different terminal neuropeptidergic fates in the Drosophila nervous system. *PloS One* **13**:e0194281. doi:10.1371/journal.pone.0194281

Hay BA, Wolff T, Rubin GM. 1994. Expression of baculovirus P35 prevents cell death in Drosophila. *Dev Camb Engl* **120**:2121–2129. doi:10.1242/dev.120.8.2121

Jackson FR, Newby LM, Kulkarni SJ. 1990. Drosophila GABAergic systems: sequence and expression of glutamic acid decarboxylase. *J Neurochem* **54**:1068–1078. doi:10.1111/j.1471-4159.1990.tb02359.x

Katheder NS, Browder KC, Chang D, De Maziere A, Kujala P, van Dijk S, Klumperman J, Lu T-C, Li H, Lai Z, Sangaraju D, Jasper H. 2023. Nicotinic acetylcholine receptor signaling maintains epithelial barrier integrity. *eLife* **12**:e86381. doi:10.7554/eLife.86381

Kato K, Forero MG, Fenton JC, Hidalgo A. 2011. The glial regenerative response to central nervous system injury is enabled by pros-notch and pros-NFκB feedback. *PLoS Biol* **9**:e1001133. doi:10.1371/journal.pbio.1001133

Kato K, Konno D, Berry M, Matsuzaki F, Logan A, Hidalgo A. 2015. Prox1 Inhibits Proliferation and Is Required for Differentiation of the Oligodendrocyte Cell Lineage in the Mouse. *PloS One* **10**:e0145334. doi:10.1371/journal.pone.0145334

Kato K, Losada-Perez M, Hidalgo A. 2018. Gene network underlying the glial regenerative response to central nervous system injury. *Dev Dyn Off Publ Am Assoc Anat* **247**:85–93. doi:10.1002/dvdy.24565

Kato K, Orihara-Ono M, Awasaki T. 2020. Multiple lineages enable robust development of the neuropil-glia architecture in adult Drosophila. *Dev Camb Engl* **147**:dev184085. doi:10.1242/dev.184085

Kolodziejczyk A, Sun X, Meinertzhagen IA, Nässel DR. 2008. Glutamate, GABA and acetylcholine signaling components in the lamina of the Drosophila visual system. *PloS One* **3**:e2110. doi:10.1371/journal.pone.0002110

Li F, Liu W-C, Wang Q, Sun Y, Wang H, Jin X. 2020. NG2-glia cell proliferation and differentiation by glial growth factor 2 (GGF2), a strategy to promote functional recovery after ischemic stroke. *Biochem Pharmacol* **171**:113720. doi:10.1016/j.bcp.2019.113720

Li G, Hidalgo A. 2020. Adult Neurogenesis in the Drosophila Brain: The Evidence and the Void. *Int J Mol Sci* **21**:6653. doi:10.3390/ijms21186653

Li Y, Gao Y, Xu X, Shi R, Liu J, Yao W, Ke C. 2017. Slit2/Robo1 promotes synaptogenesis and functional recovery of spinal cord injury. *Neuroreport* **28**:75–81. doi:10.1097/WNR.0000000000000715

Losada-Perez M. 2018. Glia: from “just glue” to essential players in complex nervous systems: a comparative view from flies to mammals. *J Neurogenet* **32**:78–91. doi:10.1080/01677063.2018.1464568

Losada-Pérez M, García-Guillén N, Casas-Tintó S. 2021. A novel injury paradigm in the central nervous system of adult Drosophila: molecular, cellular and functional aspects. *Dis Model Mech* **14**:dmm044669. doi:10.1242/dmm.044669

Losada-Perez M, Harrison N, Hidalgo A. 2016. Molecular mechanism of central nervous system repair by the Drosophila NG2 homologue kon-tiki. *J Cell Biol* **214**:587–601. doi:10.1083/jcb.201603054

Miguel-Aliaga I, Thor S. 2009. Programmed cell death in the nervous system--a programmed cell fate? *Curr Opin Neurobiol* **19**:127–133. doi:10.1016/j.conb.2009.04.002

Niu J, Yu G, Wang X, Xia W, Wang Y, Hoi KK, Mei F, Xiao L, Chan JR, Fancy SPJ. 2021. Oligodendroglial ring finger protein Rnf43 is an essential injury-specific regulator of oligodendrocyte maturation. *Neuron* **109**:3104-3118.e6. doi:10.1016/j.neuron.2021.07.018

Omoto JJ, Yogi P, Hartenstein V. 2015. Origin and development of neuropil glia of the Drosophila larval and adult brain: two distinct glial populations derived from separate progenitors. *Dev Biol* **404**:2–20. doi:10.1016/j.ydbio.2015.03.004

Purice MD, Ray A, Münzel EJ, Pope BJ, Park DJ, Speese SD, Logan MA. 2017. A novel Drosophila injury model reveals severed axons are cleared through a Draper/MMP-1 signaling cascade. *eLife* **6**:e23611. doi:10.7554/eLife.23611

Smith PJ, Howes EA, Treherne JE. 1987. Mechanisms of glial regeneration in an insect central nervous system. *J Exp Biol* **132**:59–78. doi:10.1242/jeb.132.1.59

Talifu Z, Liu J-Y, Pan Y-Z, Ke H, Zhang C-J, Xu X, Gao F, Yu Y, Du L-J, Li J-J. 2022. In vivo astrocyte-to-neuron reprogramming for central nervous system regeneration: a narrative review. *Neural Regen Res* **18**:750–755. doi:10.4103/1673-5374.353482

Yu HH, Chen CH, Shi L, Huang Y, Lee T. 2009. Twin-spot MARCM to reveal the developmental origin and identity of neurons. *Nat Neurosci* **12(7)**:947-53. doi: 10.1038/nn.2345.

Zielke N, Korzelius J, van Straaten M, Bender K, Schuhknecht GFP, Dutta D, Xiang J, Edgar BA. 2014. Fly-FUCCI: A Versatile Tool for Studying Cell Proliferation in Complex Tissues. *Cell Rep* **7**:588–598. doi:10.1016/j.celrep.2014.03.020

Figure 1

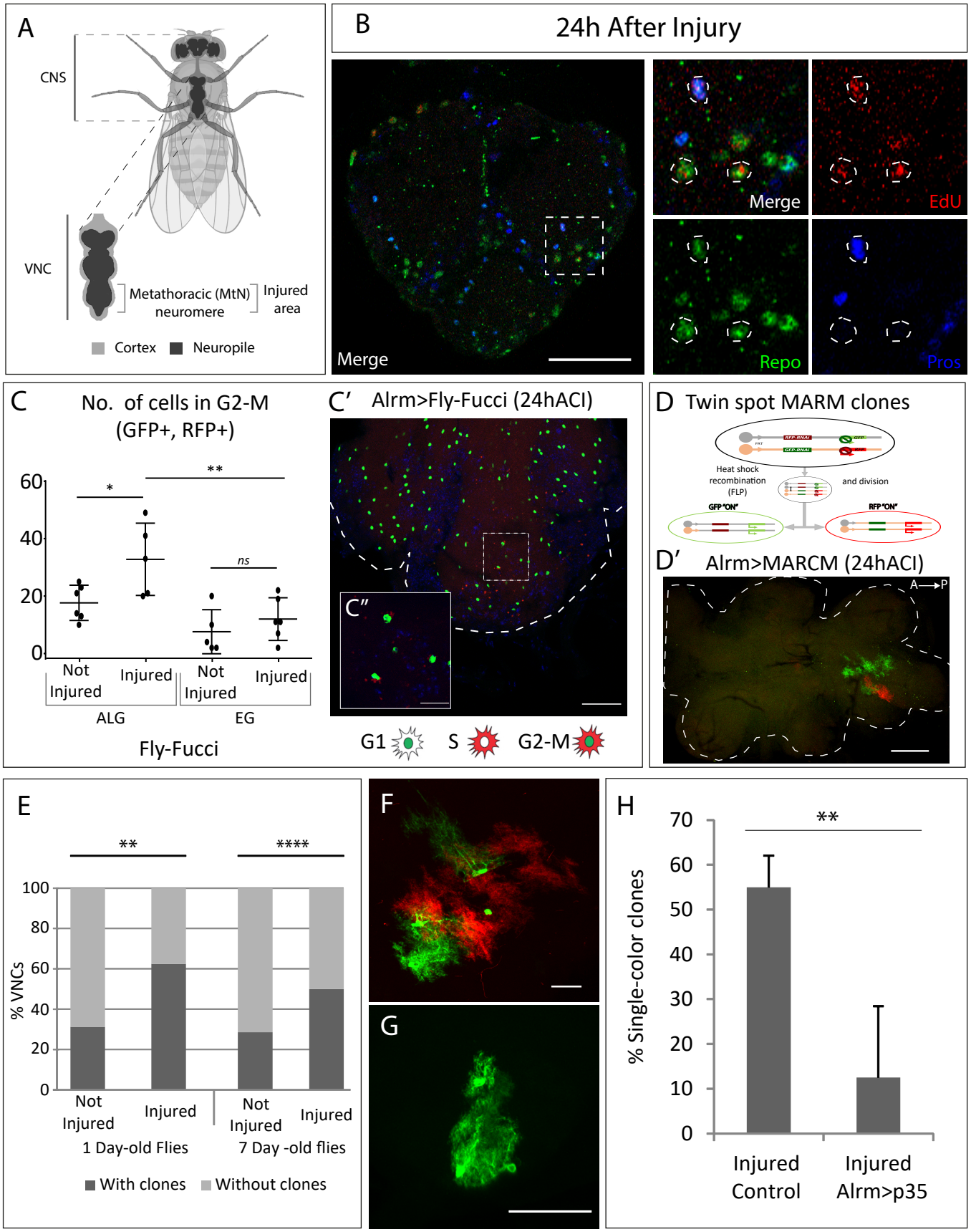
A
CNS
VNC
Metathoracic (MtN) neuromere
Injured area
Cortex
Neuropile
B
24h After Injury
Merge
Merge
EdU
Repo
Pros
C
No. of cells in G2-M (GFP+, RFP+)
60
40
20
0
*
**
ns
Not Injured
Injured
Not Injured
Injured
ALG
EG
Fly-Fucci
C′
Alrm>Fly-Fucci (24hACI)
C″
G1
S
G2-M
D
Twin spot MARM clones
Heat shock recombination (FLP)
and division
GFP "ON"
RFP "ON"
D′
Alrm>MARCM (24hACI)
A→P
E
**
****
100
80
60
40
20
0
% VNCs
Not Injured
Injured
Not Injured
Injured
1 Day-old Flies
7 Day -old flies
With clones
Without clones
F
G
H
70
60
50
40
30
20
10
0
**
% Single-color clones
Injured Control
Injured Alrm>p35

Figure 2

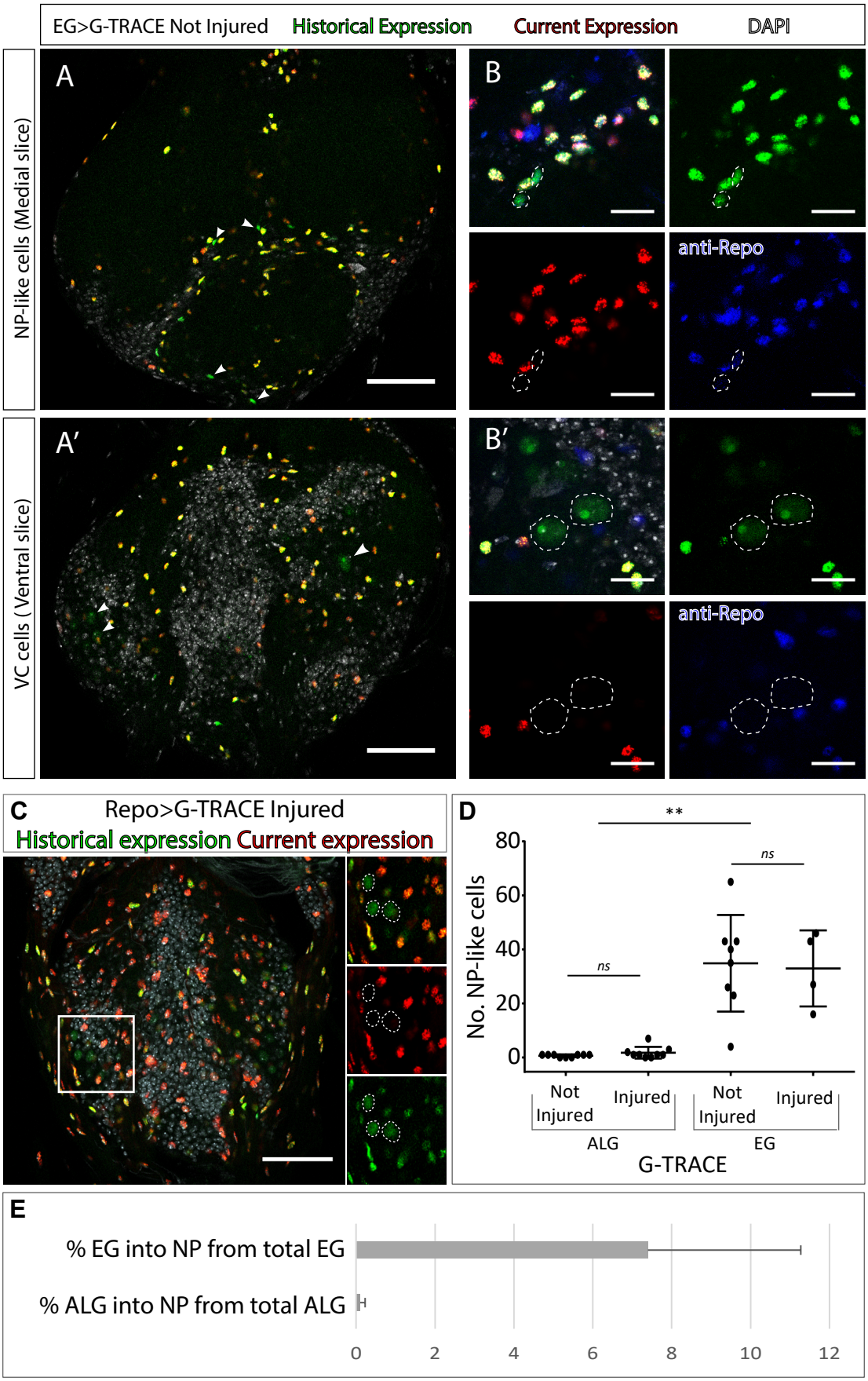
EG>G-TRACE Not Injured
Historical Expression
Current Expression
DAPI
NP-like cells (Medial slice)
A
B
anti-Repo
VC cells (Ventral slice)
A′
B′
anti-Repo
C
Repo>G-TRACE Injured
Historical expression Current expression
D
**
ns
ns
No. NP-like cells
80
60
40
20
0
Not Injured
Injured
Not Injured
Injured
ALG
EG
G-TRACE
E
% EG into NP from total EG
% ALG into NP from total ALG
0
2
4
6
8
10
12

Figure 3

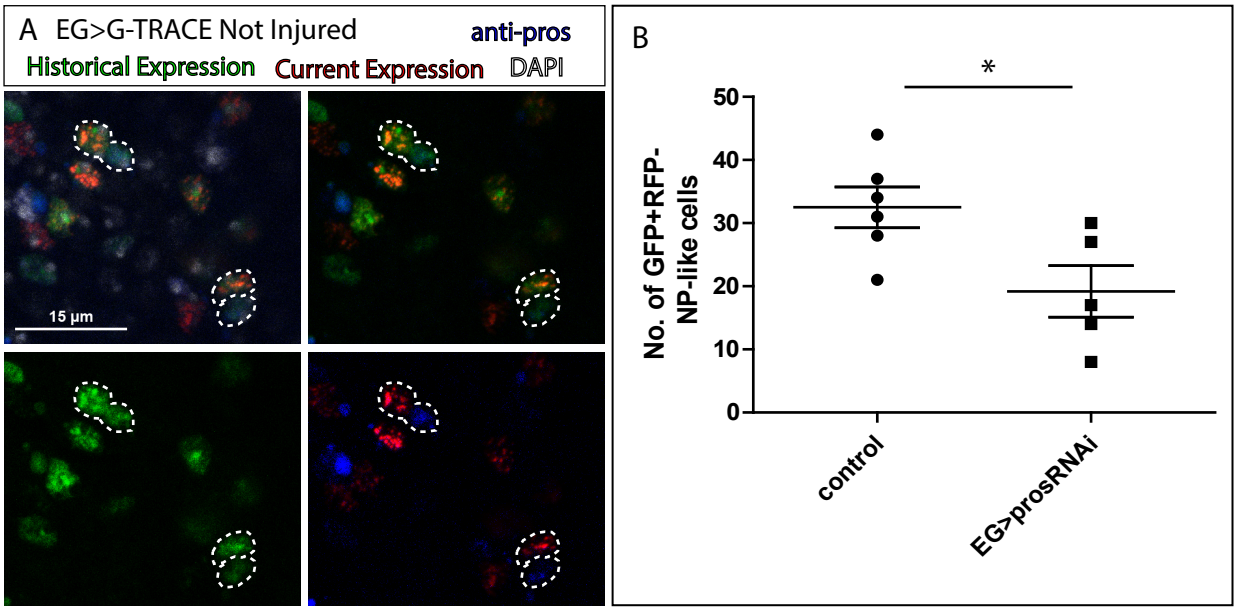
A EG>G-TRACE Not Injured
anti-pros
Historical Expression
Current Expression
DAPI
15 µm
B
*
No. of GFP+RFP-NP-like cells
50
40
30
20
10
0
control
EG>prosRNAi

Figure 4

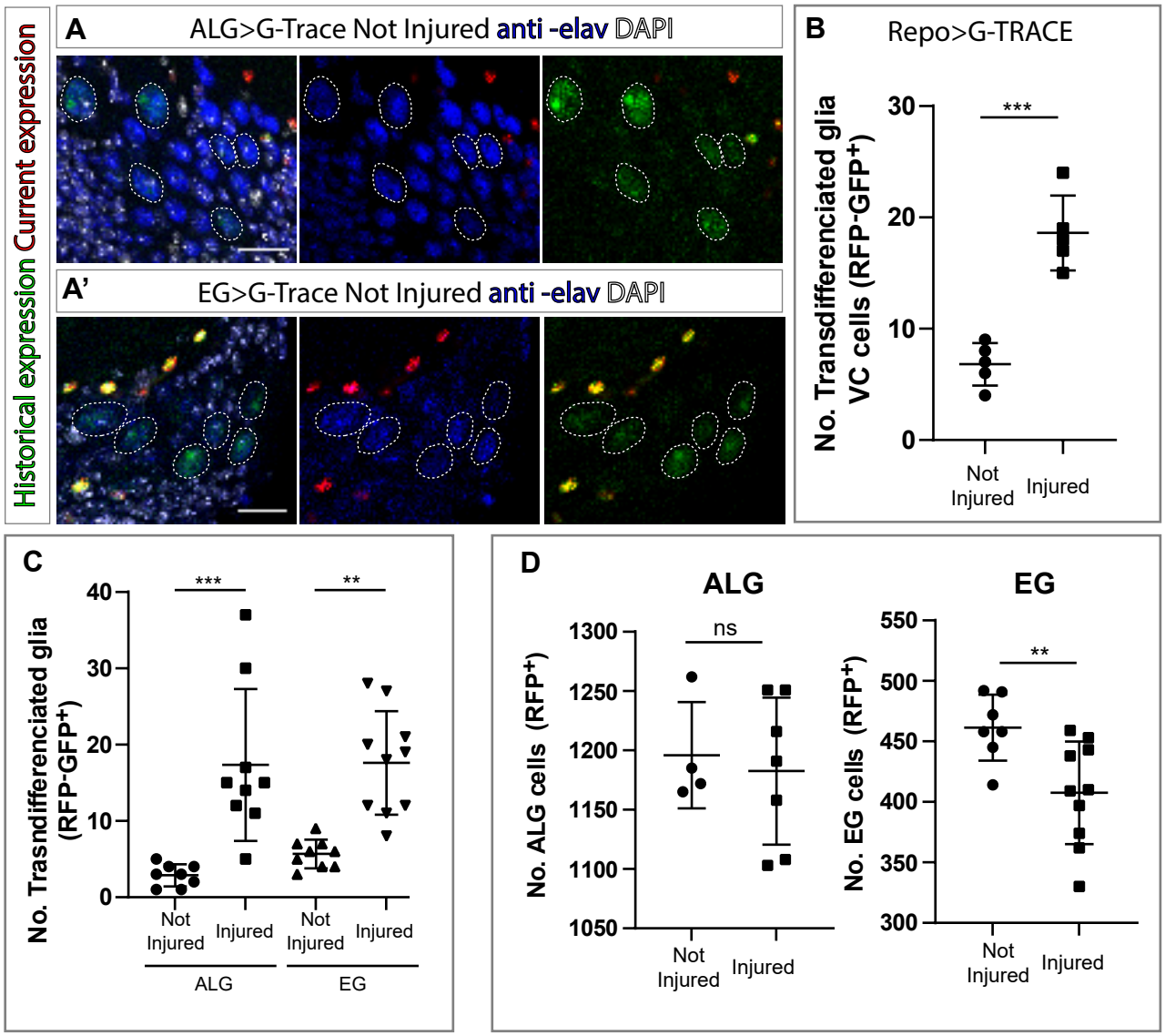
Historical expression Current expression
A
ALG>G-Trace Not Injured anti -elav DAPI
A'
EG>G-Trace Not Injured anti -elav DAPI
B
Repo>G-TRACE
No. Transdifferenciated glia VC cells (RFP-GFP+)
30
20
10
0
***
Not Injured
Injured
C
No. Trasndifferenciated glia (RFP-GFP+)
40
30
20
10
0
***
**
Not Injured
Injured
Not Injured
Injured
ALG
EG
D
ALG
EG
No. ALG cells (RFP+)
1300
1250
1200
1150
1100
1050
ns
Not Injured
Injured
No. EG cells (RFP+)
550
500
450
400
350
300
**
Not Injured
Injured